Method to Develop the Reduced Pressure Test (RPT) for Consistent Reliability and Accuracy for Everyday Foundry Operation–A Review

Robert Mackay & Glenn Byczynski
Nemak US, Southfield, Michigan, USA

ABSTRACT

The Reduced Pressure Test (RPT), also called the Vacuum Density Test (VDT), Vacuum Solidification Test (VST) or the original Straube-Pfeiffer test, has been used widely to gauge the porosity level of metal castings. The size of the aluminum casting market in the US was 11.2B USD in 2021 and much of that industry relies on the low cost and effective RPT to validate metal quality before casting. However, there can be many pitfalls in conducting the RPT due to incorrect casting of the RPT test sample and during interpretation of the results in terms melt and casting quality. This manuscript will review best practices that can support not only industry but academic institutions to incorporate the RPT more effectively in their work.

Keywords: reduced pressure test, RPT, porosity, aluminum castings

INTRODUCTION

Porosity in aluminum castings represents one of the most deleterious impacts on quality over any other defect type. It can compromise mechanical integrity and impair leak tightness capabilities which in turn results in costly scrap loss. There have been many methods to assess the liquid aluminum quality in terms of pore development prior to casting but the Reduced Pressure Test (RPT) represents the most widely used due to its low equipment cost and apparent robustness for the foundry floor. However, the methods to develop an RPT procedure and its decision-based protocols on favorable/unfavorable results is rather scant in the peer review literature or published textbooks.

An additional issue with the RPT is the general perception that the test is designed to assess the amount of gas in the liquid aluminum melt. It is now understood that oxides and dissolved H^+ collaborate to provide the thermodynamic conditions for pore development in a solidifying structure.[1-8] This means that before dissolved H^+ can contribute to pore development, oxides must be present to reduce the thermodynamic energy barrier to pore formation. Dispinar and Campbell[9] argue that pores do not nucleate via a homogeneous or a heterogeneous process but are started with a bi-film which contains encapsulated air (assumed to be 21% O_2, 78% N and 1% $H_2O_{(v)}$). The thermodynamic barrier for dissolved H^+ to diffuse into this existing air pocket is essentially eliminated and bi-film unfurling will only occur if the H_2 content in the air pocket exceeds a threshold concentration.

The chemical reactions which describe Al_2O_3 and H^+ cation generation can be shown in a still bath of liquid aluminum shown in Figure 1. During the liquid stage both H_2O vapor and O_2 in the atmosphere can react with liquid Al^{3+} to fuel Al_2O_3 formation while a continuous H^+ cation concentration buildup in the liquid will occur.

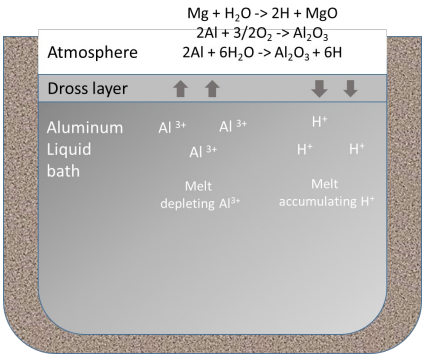

Figure 1. Schematic of the oxide layer that separates liquid aluminum and atmosphere containing H_2O vapor and O_2, the two main methods to form Al_2O_3 and H^+ generation.

During the mold filling stage, metal turbulence will result in more oxide/bi-film generation and is chemically driven by the same reactions as outlined in Figure 1. As solidification progresses the solubility drop (Figure 2) of dissolved H^+ in solid α-Al dendrites means that diffusion will readily occur into the inter-dendritic liquid providing an elevated concentration of H^+, which then are able to diffuse into encapsulated air pockets of bi-films. As H^+ diffuses into the air pocket the cations will combine to form H_2 gas which will rise the internal pressure of the air pocket and unfurl the associated oxide bi-film. At the same time the inter-dendritic liquid is gradually becoming hydrostatically stressed as volumetric contraction of the forming dendrite structure continues. Thus, it's the combined effect of the internal pressure increase due to H_2 formation and hydrostatic stress that collectively drive the growth of the pore.

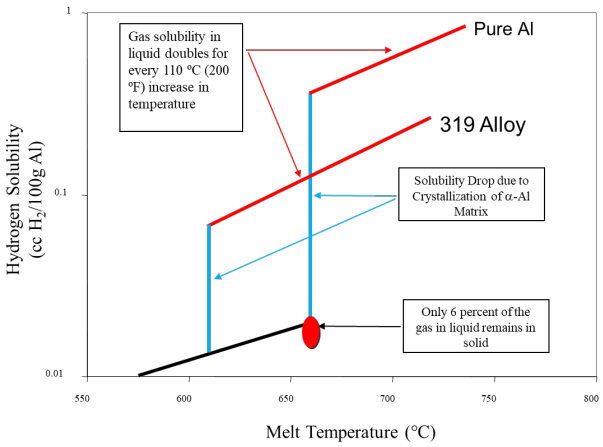

Figure 2. Solubility of hydrogen in aluminum, with 319 alloy and pure Al as examples that reflect differing solubilities.

As far as hydrogen solubility is concerned various aluminum alloys have different hydrogen absorption tendencies due to differing solubility abilities. For example, under the same conditions (i.e., melt temperature) soluble hydrogen content in the 356 alloy is 18% higher than in the 319 alloy, but 22% lower than in pure aluminum.[1,3] This is illustrated for the 319 alloy and pure aluminum in Figure 2. The hydrogen uptake can be higher at higher melt temperatures due to thermal kinetics and since the hydrogen solubility in liquid aluminum doubles for every 110ºC (198°F) increase in superheat.[1,3,4] Upon the nucleation of α-Al dendrites the solubility of H^+ drops dramatically and must defuse into the remaining inter-dendritic liquid.

The equipment to gauge porosity severity in aluminum melts is somewhat numerous and only capable of measuring dissolved H^+ levels or capable of measuring existing oxides or inclusions, but usually not both. Keep in mind that oxides and inclusions detected from liquid aluminum samples were in the holding bath previously and these methods do not assess the number of oxides generated during the mold filling event, many of which will form the ideal bi-film configuration more so than the turbulence associated with liquid processing (e.g., rotary degassing).

Table 1 lists most of the known commercial equipment used to assess melt quality. The red "X" simply means that the technologies highlighted in Table 1 are only capable of assessing either oxides or dissolved H^+, not both. The yellow check marks for the RPT reflects that the system derives a result based on both oxides and dissolved H^+, just that it cannot distinguish magnitudes between the two.[3,7,9]

Table 1. Commercial Equipment Available for Melt Quality Assessment

Equipment		Oxides or Inclusions	Dissolved Hydrogen
Alspek		✗	✓
Alscan		✗	✓
HYSCAN		✗	✓
Sialon Ceramics		✗	✓
LiMCA		✓	✗
PoDFA/Prefil		✓	✗
MetalVision		✓	✗
ALMEX		✓	✓
Reduced Pressure Test		✓	✓

Direct hydrogen analyzers, such as Alspek, Alscan, Hyscan, etc., are better suited to understand dissolved H^+ concentrations and degassing characteristics of the liquid aluminum in breakdown and holding furnaces prior to the casting process. Inclusion/oxide analyzers such as PoDFa/Prefil, MetalVision and LiMCA do not directly assess dissolved H^+ concentrations but can quantify/qualify inclusion and oxide content of the melt. The ALMEX system is something the authors have not used but it's reported to be able to conduct both tests in upper and lower portions of its setup. The RPT test can directly assess porosity severity, but it cannot identify the contributions of dissolved H^+ or existing oxides to the porosity observed in the RPT sample.[3] An additional point that needs to be made about the RPT is that the shorter training time and resources required allows for floor operators to functionally and reliable conduct the test. All the other equipment listed in Table 1 is better suited to be operated by employees with metallurgical expertise.

Owing to the low equipment cost and relatively short training cycle needed to conduct the RPT it's expected that this will be the primary front-line tool used in most aluminum cast shops in the USA for some time to come. However, as the range of compositions within the Al-Si-Cu family grows, each having a slightly different absolute density and freezing ranges, using reference data may not provide the accuracy needed for today's aluminum

foundry. The three key questions to be answered in this manuscript are:

1. How does one establish the absolute density, especially for Al-Si-Cu alloys which have limited previous reference data?
2. As the absolute densities and freezing ranges for alloys within the Al-Si-Cu family are different, what factors are considered in establishing a production valid density threshold?
3. Is there an understanding of what factors can control false positives or false negative results in terms of the density threshold (± 0.01 g/cc)?

EXPERIMENTAL METHODOLOGY–RPT PROCEDURE

A brief description of the equipment setup for the RPT sample collection will be reviewed. The fundamental aspect of the RPT is that a sample of liquid aluminum is allowed to solidify in a reduced atmospheric condition (Figures 3a and 3b). As pores begin to form, the effect of the low atmosphere is that the internal gas pressure can dominate growth kinetics to the point where pores become much larger, and thus enhances one's ability to assess pore formation tendencies.[1-8]

Notice from Figure 3a that there are two vacuum gauges, while many RPT units have only one. This is important as the second vacuum gauge on top of the dome prevents the continuation of a test where the dome sealing rim is compromised. Secondly, the operator can view both vacuum gauges to see if there is a lag, which would also be due to dome sealing irregularities.

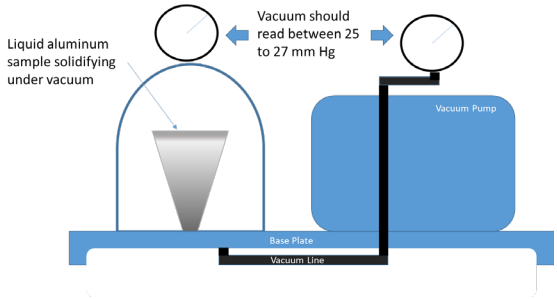

Figure 3a. Representation of the RPT apparatus with champagne cup.

There are two general cup designs that seem to be used and are referred to the *champagne cup* geometry and the *muffin cup* geometry. The authors have used the champagne cup in this manuscript. In a dry mass check of 60 RPT samples an average mass reading of 122.6 ± 7.8 grams was found. This will be important as the size/mass of the RPT sample will dominate the overall solidification time. However, it's expected that all the practices and observations will be replicated for both cup geometries.

Figure 3b. Image of the RPT hardware used at Nemak. (Artwork courtesy of Palmer Manufacturing.)

The muffin cup geometry example is approximately 40 grams more massive and promotes a slightly longer solidification time which needs to be kept in mind as both the solidification time and mass of the RPT sample will be shown to be critical to establishing accurate RPT densities. The schematic of both cup designs and their respective mass values are reflected in Figure 3c.

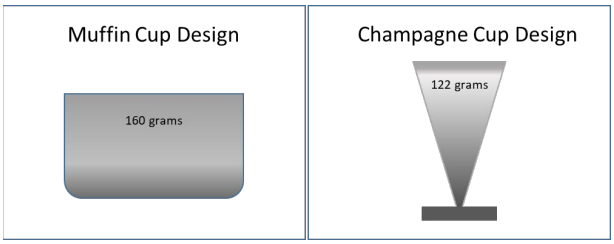

Figure 3c. Schematic of the RPT sample mass in the muffin cup and the champagne cup geometries. Mass does not include the cup itself.

The champagne cup will be used in this manuscript as it is the cup design used to support the production of several casting lines the authors have commenced over the last 15 years.

PRE-CAST PROCEDURE:

Figure 4 outlines the steps used to ensure the correct and repeatable procedure for the RPT. The rationale used for each of these steps will now be reviewed.

One of the most critical elements that may be missed is the RPT cup pre-heat to promote the liquidity of the sample long enough before the dome is placed on the insulating base of the RPT unit, and the vacuum is started.

1. First, suspend the RPT cup above the melt bath to drive off moisture before there is any contact with liquid aluminum (***Step 1***).
2. Next, immerse the cup into the liquid bath, but not below the cup rim, and when the exposed portion of the cup shows a cherry red appearance it can be removed and placed on the cup stand of the RPT unit (***Steps 2 & 3***).

3. Finally, with a ladle, pre-heat for moisture removal and then immerse the ladle to collect liquid aluminum and transfer into the cup, filling it to the rim (***Step 4***).
4. Immediately place the dome on top of the sample and ensure that the target vacuum is reached on both vacuum gauges (-25 to -27 mm Hg) (***Step 5***).

SOLIDIFICATION DURING RPT

To ensure that the solidification time is adequate it's important to first understand that many of the alloys within the Al-Si-Cu family will have different solidification times and freezing ranges.[1] To ensure that complete solidification occurs the Secondary Dendrite Arm Spacing (λ_2) array is measured in sectioned & polished RPT samples as shown in Figure 5. From there one can use the relationship between solidification time and λ_2, where $\lambda_2 = 10.85t_f^{0.30}$, t_f is solidification time between $T_{liquidus}$ to $T_{Solidus}$ and was established for a range of Al-Si-Cu alloys.[10] From Figure 5 we can also determine that the time for solidification of the RPT sample should be set at 4 minutes, not 3.8 minutes as that is when $T_{solidus}$ was achieved (***Step 6***). However, when a foundry or institution uses the RPT they should run through this exercise to ensure that complete solidification is reached before the vacuum is turned off. For example, if the muffin cup geometry (approximately 40 grams heavier) is used, the solidification times will exceed the 4-minute window established for this alloy. Also, should a slightly different Al-Si-Cu alloy be used the overall freezing range (solidification time) will also be different and necessitate the λ_2 array analysis as in Figure 5. More specifically, increasing Si concentrations will do the most to extend solidification times owing to the 5 times latent heat evolved from Si platelets when compared to dendritic or eutectic Al.[1] Figure 6 is a confirmation of the solidification profile repeats with a non-degassed metal sample (2.54 g/cc) and after the same metal bath was degassed (2.72 g/cc).

It is possible to use a longer blanket solidification time for the RPT which would cover all alloy compositions and cup geometries/size. This would depend on the frequency the test is done per casting line and on the number of casting lines which require RPT monitoring. The authors have in-plant experience with three casting lines, requiring a total of 6 RPT samples to be taken per line in a 24 hour period. This totals 18 RPT samples and if a longer solidification time of 7 minutes for each test was used, this would add 54 minutes to the daily requirement for RPT sampling by the operator.

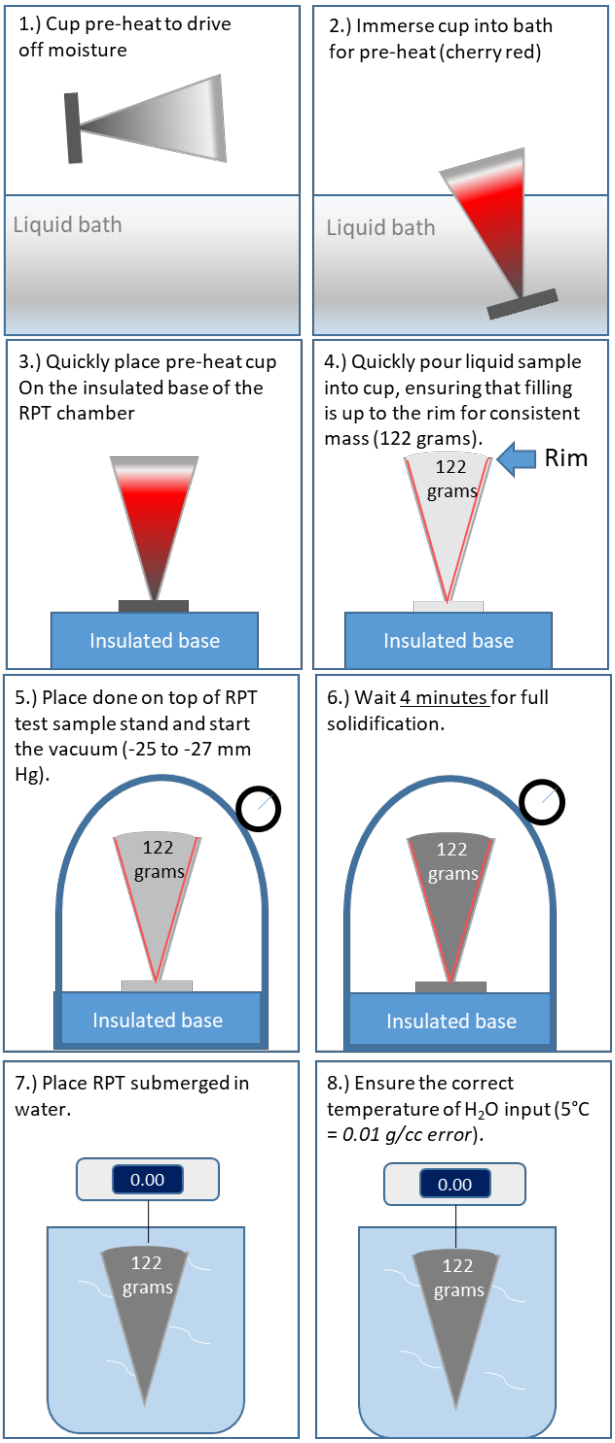

Figure 4. The critical steps for casting a consistent RPT sample. Most critical is the pre-heat of the cup via in bath emersion and quickly filling the liquid metal to the rim. The pre-heat ensures a slower solidification while filling to the rim ensures that sample mass is ~122 grams.

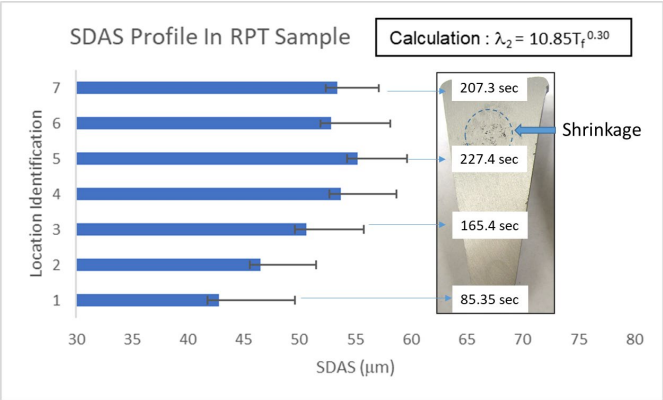

Figure 5. A baseline solidification profile of an RPT test sample. Solidification times are estimates but are calculated based on the above mathematical relationship developed for the alloy in question. The 5th location has the longest solidification time of 3.8 minutes.

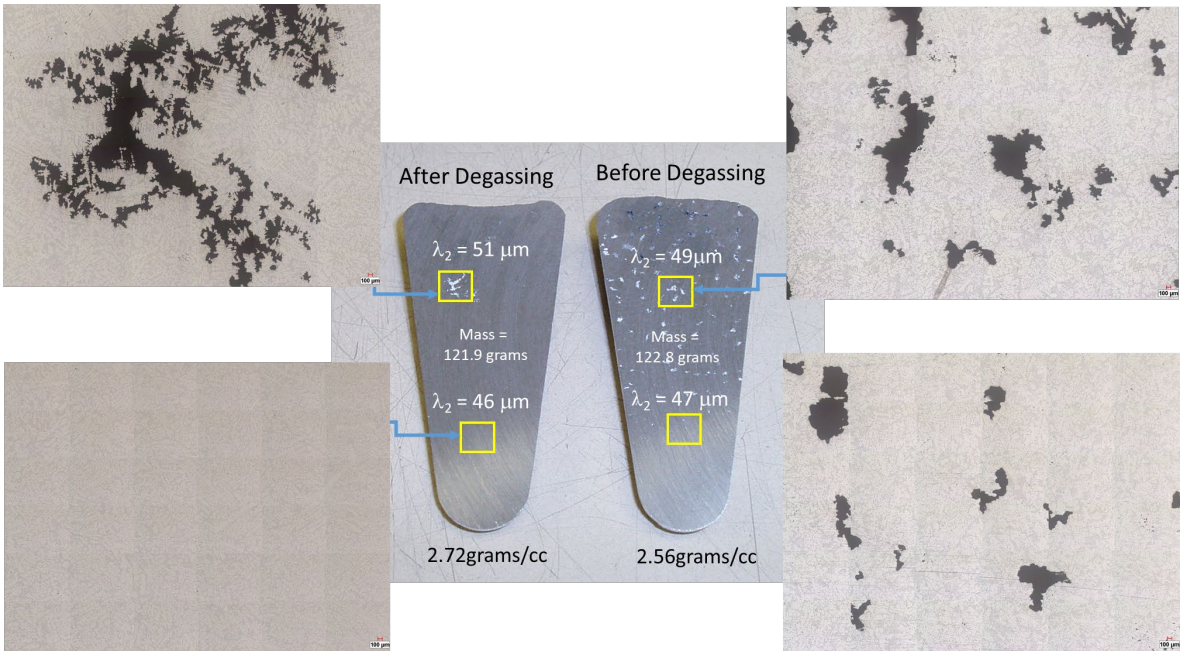

Figure 6. Similar benchmark of solidification rates in degassed and non-degassed liquid aluminum. As with the benchmarking sample in Figure 5 only a single gross shrinkage pore is seen in the degassed metal. The RPT sample mass is also listed in the figure.

AFTER SOLIDIFICATION OF THE RPT

After solidification, the sample is placed into a programmable balance unit which provides a direct calculation of the relatively density. The calculation for relative density is shown in Equation 1.0.

$$\rho_a = \frac{W_a \rho_w}{(W_a - W_w)} \qquad (1.0)$$

Where ρ_a = relative density, W_a = dry weight, W_w = wet weight and ρ_w = density of water which is temperature dependent.

While there would normally be less potential variation in this stage of the RPT process there are two critical factors to ensure proper reading. First, ensure that the RPT sample is completely immersed below the waterline (***Step 7***). Should that sample be partially above the water line, the calculated relative density result would be higher than actual. Second, ensure that the water temperature is measured accurately as an error of up to 5°C (9°F) will translate into a 0.01g/cc error in density reading (***Step 8***).

EXPERIMENTAL METHODOLOGY– DEVELOPMENT OF ABSOLUTE DENSITY

The final aspect to review for the RPT development is the method to easily determine the absolute density (theoretical density) of the alloy when dealing with Al-Si-

Cu compositions which are unique and without reference alloy density data. The authors use a straightforward process and is outlined as follows: Using the same programmable balance unit for the RPT, one can use a known low porosity value of the same alloy to find absolute density. An example that is very easy to conduct in-house is to use the Optical Emission Spectrometer (OES) production sample of the alloy in question. The OES samples measured for this work have a value of λ_2 at 20−22 μm, with no measurable porosity from image analysis systems. The OES samples must solidify extremely fast so that a chemically homogenous sample (limited segregation) is achieved.

EXPERIMENTAL METHODOLOGY–CASTINGS USED TO SUPPORT RPT DEVELOPMENT

In addition to the RPT samples that will be studied in this manuscript, a series of castings were made at two different RPT densities (non-degassed–2.66 g/cc and after degassing–2.70 g/cc). The chemistry of the specific alloy (Alloy 1) that will be used is shown in Table 2. This alloy does not have an AA designation nor is used widely except for specific applications in internal combustion engines.

Table 2. Chemistry of Al-Si Cu Alloy Test Castings (wt.%)

Alloy 1	Si	Cu	Mg	Mn	Fe	Zn	Sr	Ti	Ni	Pb	P	Cr
Max	8.75	2.95	0.4	0.44	0.59	0.8	0.007	0.16	0.14	0.05	0.002	0.1
Min	8.1	2.6	0.31	0	0.27	0.4	0	0	0	0	0	0

These castings will be used to understand quality in terms of microscopy (porosity) and the resulting mechanical property condition. The total number of castings used at both RPT density levels will be 30 to support the minimum statistical requirement for Weibull modulus determination. Also, the same mechanical property data will be shown as simple average values with standard deviation, and Quality Index (Q = UTS + 150LogE) calculation.[3]

Tensile testing (ASTM E8) was used to assess the mechanical property response to the measured RPT density level. Tensile test bars were extracted from a chilled section of a precision sand casting which has a refined microstructure (λ_2 = 25 to 35 μm). Tensile sample fabrication and testing was conducted by an accredited metallurgical lab under ISO/IEC 17025 by A2LA.

Light Optical Microscopy (LOM) was conducted on completed tensile test samples for both λ_2 determination, the mean percentage porosity and maximum pore found from a 7mm x 7mm grid containing 49 fields. The grid was 1 mm below the fracture surface to link LOM results with mechanical performance.

Finally, the last section to solidify is in the casting sections next to the risers (λ_2 = 55 to 60 μm). It is presumed that the extend of the porosity development will be the highest due to the longer solidification times which allows more H^+ diffusion into unfurling bi-films. The porosity resulting in this coarse region will be assessed via LOM imaging examples followed by the resulting radiography grade (ASTM E155).

RESULTS

BASELINE RPT SAMPLE SETUP

From the λ_2 array in Figure 5 we can see that the final stage to solidify is where the gross shrinkage is located (hot spot). Using the relationship between λ_2 and solidification time one can established that the longest time to solidify in the RPT sample is 227.4 seconds, or 3.8 minutes, to reach solidus.

For RPT repeatability in terms of solidification time it becomes critically important to ensure adequate pre-heat of the champagne cup and transfer ladle, and the size of the RPT sample poured must be the same. Maintaining the tightness of the mass is made somewhat easy as the practitioners pour the samples up to the cup rim every time. The effect of pouring undersized samples means that solidification times maybe shorter and potentially produce an overestimate of the density result.

Figure 6 showed the spot check (locations 6 and 2 in Figure 5) for λ_2 in two locations in an RPT sample reading 2.56 g/cc in Alloy 1 (Table 2), and then after degassing and achieving a 2.72 g/cc reading. The λ_2 values are identical reflecting the fact that the solidification times are essentially identical due to both the consistent sample masses (122.8 grams in non-degassed metal and 121.9 grams in degassed metal), and by the fact the RPT cups were pre-heated beforehand. However, the density is almost 6% lower in the non-degassed alloy. This is reflected in the upward concavity of the top surface of the non-degassed sample, while the degassed sample concaves downward. The top-surface upward concavity is due to the much larger volume of porosity within the RPT sample.

IMPACT OF ALLOY CHEMISTRY & DENSITY THRESHOLD DETERMINATION

So far there has been no discussion on the method to properly setup a threshold density for similar alloys within the Al-Si-Cu family. For example, the 319 alloy typically, as seen by the author in both academic and industrial settings, a blanket 2.70 grams/cc threshold is used, and many sources cite 2.79 g/cc as its absolute density.[3,6] Yet within the Al-Si-Cu alloy family there is very wide range in Si and Cu compositions, which changes not only the H^+ solubility in α-Al dendrites of the

alloy, but also freezing range and solidification time, on the final density reading.

As discussed in the section: Experimental Methodology–Development of the Absolute Density, using a programmable balance unit may provide a quick answer by using an OES sample if it is a known pore-free sample. Table 3a shows this exercise conducted on two Al-Si-Cu alloys (which includes Alloy 1 used to manufacture the test castings in this study) used for precision sand castings to make engine blocks, and three pure metal samples (Zn, Tn and Cu) in Table 3b.

Table 3a. Chemistry Limits for Two Al-Si-Cu Alloys Used for Engine Block Manufacturing and Absolute Densities from Production OES Samples (wt.%)

	Si	Cu	Mg	Mn	Fe	Zn	Sr (ppm)	Density of OES Sample
Alloy 1	8.75	2.95	0.4	0.44	0.59	0.8	65	2.74 g/cc
	8.1	2.6	0.31		0.27	0.4	0	
Alloy 2	7.8	3.7	0.35	0.3	0.4	0.25	20	2.76 g/cc
	7.2	3.3	0.25	0.2	0	0	0	

Table 3b. Absolute Density Determination for Pure Zn, Tn and Cu using the Programmable Balance Unit

Pure Eleme	Periodic Table	Absolute Density	Agreement
Zn	7.09 g/cc	7.13 g/cc	99.60%
Tn	7.26 g/cc	7.31 g/cc	99.90%
Cu	8.49 g/cc	8.96 g/cc	99.20%

Using the programmable balance unit on the OES samples to derive the absolute densities seems reasonable. Using the pure pore-free elements in Table 3b we see that periodic table agreement is well above 99%. One further point needs to be made from the results of Table 3a. The absolute densities seen will most likely never be achieved in the RPT sample from a well degassed melt. This is due to the geometry of the champagne cup where the solidification rates between the exposed top and the mid-section shows a hot spot where microshrinkage is forced to form. After establishing the absolute density of 2.74 g/cc for Alloy 1 an estimated 25K RPT samples covering a production run of 15 years were cast and the highest reading ever captured was 2.72 g/cc. The muffin-shaped geometry cup is wider and may have more favorable feeding conditions that better deters any hot spots from occurring when compared to the relatively long and slender champagne cup.

Now that the density of essentially pore-free alloy is known, what threshold should be used to produce acceptable quality castings? The next stage of the RPT development is to run casting trials with more than one RPT result.

DEVELOPMENT OF RPT THRESHOLD FOR PRODUCTION

Developing a threshold density value that results in acceptable castings is critical to establish, but this value may not be the same for all casting processes which use the exact same alloy. Two groups of castings, totaling 30 each, were made with a low and high RPT density value. The lower value can be achieved by not degassing the melt ahead of time and then pouring the 30 castings (2.66 g/cc). Then pour another 30 castings after degassing to a set target (2.70 g/cc). With both casting groups perform quality checks in the fine and coarse microstructure regions for all 60 castings. The details of these results are outlined in the next section.

CASTING DEVELOPMENT FOR RPT THRESHOLD IN FINE MICROSTRUCTURE REGIONS (L_2 = 25 to 35 mm)

Tables 4a and 4b shows the data summary for 60 development castings made with Alloy 1, with 30 casting made with metal non-degassed having a 2.66 g/cc reading, and another 30 castings degassed with metal to 2.70 g/cc, to support final casting development at the Production Part Approval Process (PPAP) stage. Specifically, Table 4a lists the metallographic data summary from the completed tensile test bars (1 mm below fracture surface), and Table 4b summarizes the average tensile properties for yield strength (YS), ultimate tensile strength (UTS) and elongation (E), and from a calculated Quality Index (Q).

Table 4a. Microstructural Data from Tensile Test Bar Extracted from Casting in a Refined Microstructure Area of Engine Block (n = 10 for each density level)

Iteration #	Metallography & Microhardness 1 mm below tensile test sample fracture surface		
	λ_2 [µm]	Porosity [%]	Max Pore [mm]
RPT = 2.66 g/cc	32.6 ± 2.1	1.0 ± 0.4	360.2 ± 146
RPT = 2.70 g/cc	31.1 ± 2.4	0.42 ± 0.11	251.5 ± 97

Table 4b. Summary of Average Values for UTS, YS, PE and Q of the engine block with 2 RPT values–bulkhead (n = 30 for each density level)

Iteration #	Tensile Test (ASTM E8 Protocol)			Quality Index (Q = UTS + 150 LogE) [MPa]
	Yield [MPa]	UTS [MPa]	Plastic Elongation [%]	
RPT = 2.66 g/cc	244.5 ± 5.6	272.1 ± 12.3	0.40 ± 0.12	212.3
RPT = 2.70 g/cc	245.4 ± 6.1	280.8 ± 9.7	0.61 ± 0.15	247.7

In Table 4a the percentage porosity and max pore found from tensile test bars extracted from bulkhead casting sections made with non-degassed liquid metal (2.66 g/cc)

are higher than for the same tensile test bars extracted from castings sections made with degassed liquid metal (2.70 g/cc). Table 4a also shows that the λ_2 values measured from the tensile test bars with both groups of castings are essentially identical, meaning no changes in solidification rates were encountered which would skew the porosity comparison erroneously.

Table 4b shows that there is little change in the average values for mechanical properties except for the average ultimate tensile strength (UTS) which is slightly lower with a higher standard deviation in the 2.66 g/cc non-degassed metal. However, the Quality Index (Q) is also calculated in Table 4b and shows a higher value from the melt quality of the 2.70 g/cc dataset.

Using the raw mechanical property data in Table 4b we can plot histogram distribution plots and Weibull modulus as shown in Figures 7a-d. Figure 7a shows the frequency distribution of elongation values, and Figure 7b for the frequency distribution in UTS, for castings made with 2.66 g/cc metal and the castings made with 2.70 g/cc metal, respectively. Unlike the result of Table 4b, there are separations in elongation and UTS values which can be seen more distinctly. The lower values of elongation and UTS seen with 2.66 g/cc non-degassed metal, not buried within an average calculation, shows that there are some individual tensile test results which are much lower in value that for the tensile test results from 2.70 g/cc treated metal.

Figures 7c and 7d show the Weibull plots for the elongation and UTS and the Weibull modulus value is clearly higher for castings made with metal degassed to 2.70 g/cc. The higher modulus makes sense as elevated porosity will normally not affect yield strength (YS) significantly but will provide a drop in elongation and UTS.

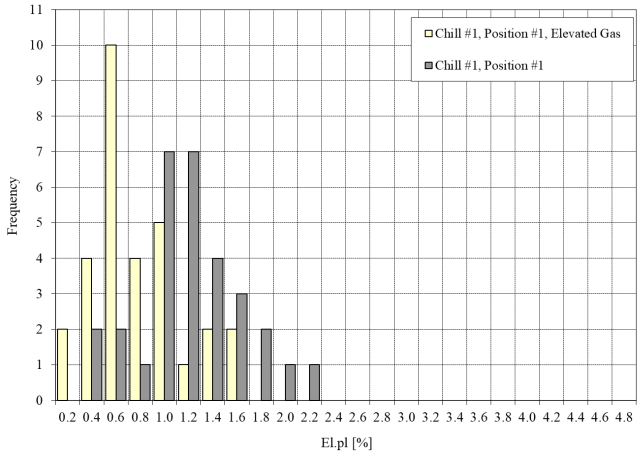

Figure 7a. Frequency plot of elongation values with casting poured with melts at 2.70 g/cc and 2.66 g/cc.

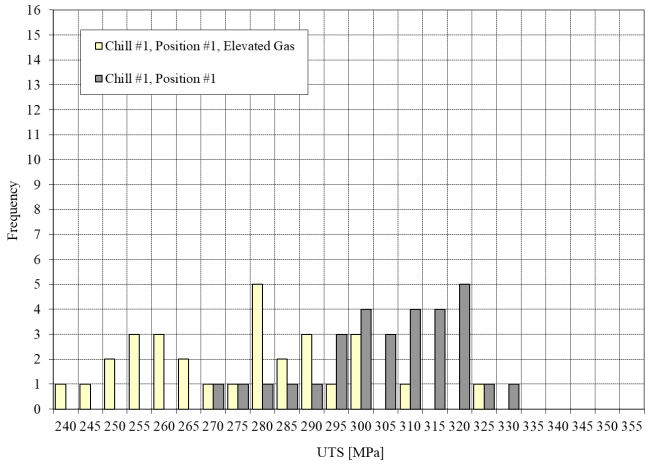

Figure 7b. Frequency plot of UTS values castings poured with melts at 2.70 g/cc and 2.66 g/cc.

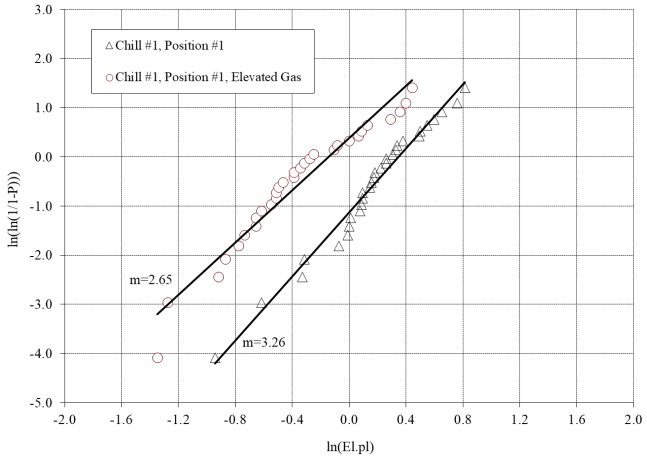

Figure 7c. Weibull plots for elongation. The Weibull modulus changes from 2.65 for 2.66 g/cc non-degassed metal to 3.26 for 2.70 g/cc treated metal.

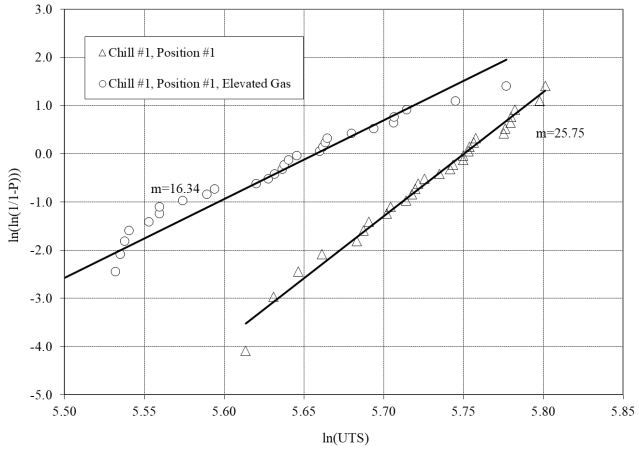

Figure 7d. Weibull plots for UTS. The Weibull modulus changes from 16.34 for 2.66 g/cc non-degassed metal to 25.75 for 2.70 g/cc degassed metal.

CASTING DEVELOPMENT FOR RPT THRESHOLD IN COARSE MICROSTRUCTURE REGIONS (L_2 = 55 to 60 mm)

Normally automotive castings are machined, and finished surfaces may reveal what is know as salt and pepper porosity which can affect sealabilty of mating surfaces and/or promote a leak path that impairs pressure tightness. Figures 8a and 8b show micrograph images of machined features from the coarse region (λ_2 = 55 to 60 µm) from the castings made at 2.70 g/cc and 2.66 g/cc, respectively.

Metallography was used to ensure that the porosity could be fully revealed. This evaluation being conducted only on a machined surface can underscore porosity severity as some of the smaller pores will have plastic smearing into the openings. In radiography this porosity can also be assessed using the ASTM E155 standard via the P-rating level (ranges from 0–8, where 0 shows no dispersed microporosity). The G and S ratings within the ASTM E155 radiographic standard were not observed to increase in size or frequency, but it's presumed that the H^+ concentrations are not high enough as pores characterized as G rated usually form very early during solidification and are associated with improper filling or interrupted filling of the mold, and S ratings are related to shrinkage defects (hot spots) which also would require more dissolved hydrogen to increase the size.

The LOM seen in Figure 8a is from the coarse regions of the casting (adjacent to risers) and made with metal degassed to 2.70 g/cc. The ASTM E155 radiographic rating for this region was P3, while in Figure 8b, showing the same casting location except made with 2.66 g/cc non-degassed metal, had a radiographic rating of P5. Also, highlighted in Figure 8b are three pores in excess of 0.5 mm in diameter and are the same pores which contribute to salt and pepper porosity seen on machined surfaces.

No changes to the casting process for both casting groups occurred except for the RPT result, meaning that the level of suspended oxides before pouring (captured by the RPT), and bi-film formation during filling, was the same due to the target fill times for the casting (25 sec.).

Referring to Table 4b we could see that only a small difference in average value of the UTS between the two RPT groupings could convey that operating as low as 2.66 g/cc was permissible, and after all this may represent a lower cost for manufacturing. The additional development work utilizing the Quality Index, and the Weibull statistical method in terms of fine microstructural regions of the casting reveal that 2.66 g/cc was not correct. In coarse microstructural regions it became more obvious that 2.66 g/cc would not work based on the elevated P-rating in radiographic data.

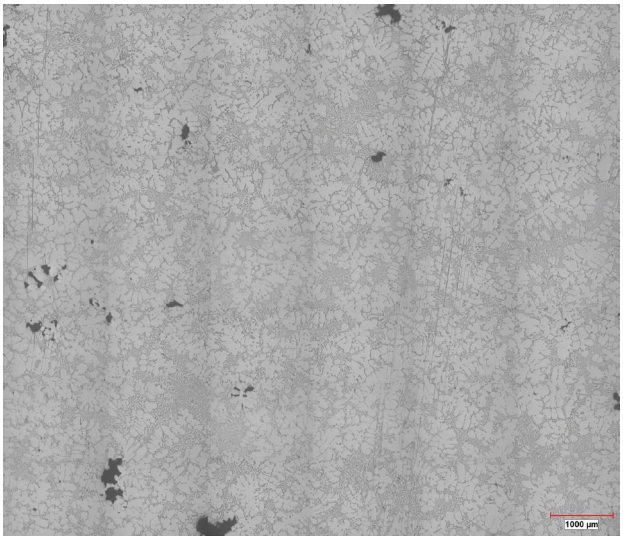

Figure 8a. LOM of the coarse regions (l2 = 55 to 60 mm) form in a casting made with 2.70 g/cc degassed metal had an ASTM E155 P rating of 3. Most of these pores would be covered up by plastic smearing into the pore openings during machining.

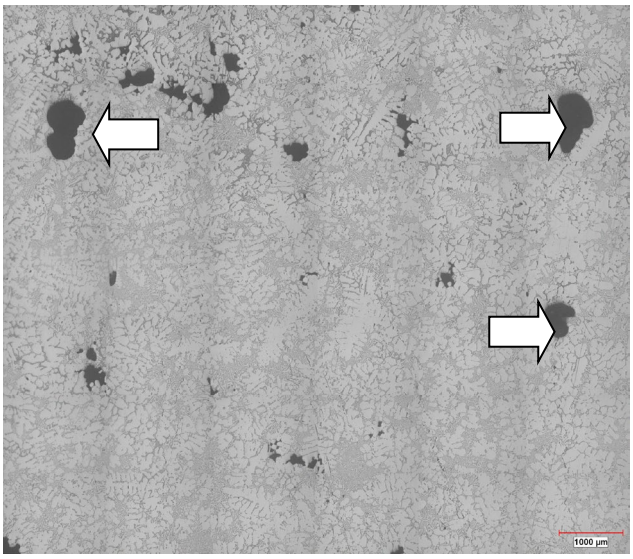

Figure 8b. LOM of the coarse regions (l2 = 55 to 60 mm) form a casting made with 2.66 g/cc non-degassed metal had an ASTM E155 P rating of 5. Three large pores (≥ 500 mm, indicated by white arrows) most likely would show up on a machined surface. The balance of pores may be filled in plastically during machining.

In short, the acceptable range for RPT data for higher quality and compliant castings, using Alloy 1, is 2.70 g/cc to 2.74 g/cc, where using the champagne cup geometry this range will practically be 2.70 g/cc to 2.72 g/cc.

DISCUSSION

This manuscript set out to show a valid method for the development of the RPT and then to match it appropriately to the intended casting process. This approach has been used by the authors for some time in manufacturing so that a dependable RPT reading is achieved, allowing production to run effectively and support the lowest manufacturing costs. As mentioned, the US aluminum metalcasting industry is valued at 11.2B USD (2021) and much of that industry relies on the RPT to qualify the melts acceptability to cast. Yet there have been misconceptions that the RPT truly measures gas only, and some of the reference threshold densities found, and their absolute densities, appear to be similar for a range of Al-Si-Cu alloys, which if applied, may not be correct for the intended process.

There are other precision sand castings which use Alloy 1 and are smaller in size (castings with rigging) which may have faster solidification times and thus may permit a slightly lower RPT threshold value. For example, another engine block casting which used the same alloy and same casting process but was 36% lighter (solidified faster and was reflected by lower λ_2 values), can use a 2.68 g/cc threshold based on the same extensive casting evaluation used in this manuscript. This can reduce the number of inert rotary degassers, filtration and setting times required before casting.

For the Gravity Semi-Permanent Mold (GSPM) it has been seen that the thresholds in RPT density appear to be similar to what is used for the Precision Sand Casting Process (PSCP) because the largest coarseness in microstructure is similar (e.g., $\lambda_2 \sim 50$ to 60 µm). For the High Pressure Die Casting (HPDC) process the thresholds in RPT density are even lower, some near 2.60 g/cc. This has nothing do due with the alloy (typically 380 and 383 alloys) as their freezing ranges are not significantly different to other Al-Si-Cu alloys or is there a large difference in H^+ solubility, but that inherent in the HPDC process is the speed at which mold filling occurs, and how fast solidification rates are (e.g., $\lambda_2 \sim 20$ to 30 µm). Unlike the PSCP, which has mold filling lasting for up to 25 seconds, HPDC has mold filling within fractions of a second. The oxide generation and subsequent folding that occurs with a fast metal filling process contributes to much higher casting porosity which has nothing to do with metal quality.

The development process for the RPT outlined in this manuscript can be used to support all the casting processes just outlined. The 30 castings were needed to extract the 30 tensile test bars to support the Weibull statistical requirement. Both PSCP and GSPM will adequately provide statistically relevant mechanical property response with 30 castings, but for HPDC, depending on the porosity severity, may require more castings to be sacrificed as the scatter in tensile results are much higher.[1,11]

Finally, this manuscript reviewed the elements required to conduct a repeatable RPT with a complete discussion on how errors can occur in the resulting final density reading. Figure 9 is a representation of the types of errors which can occur in terms of false positive densities and false negative densities. Using Figure 9, should a melt quality operator get a 2.69 g/cc RPT result, check that any of the factors that could falsely produce a 2.69 g/cc reading are ruled out before stopping production. In this case start by ensuring the dry weight of the RPT sample is within traditional ranges of 122.6 ± 7.8 grams, and that the water temperature is correct in the density calculation. Should the dry weight and water temperature be found to be accurate then a second confirmatory RPT should be taken. Should the reading still be 2.69 g/c then it's safe to say that there is a process deviation occurring with liquid metal treatment.

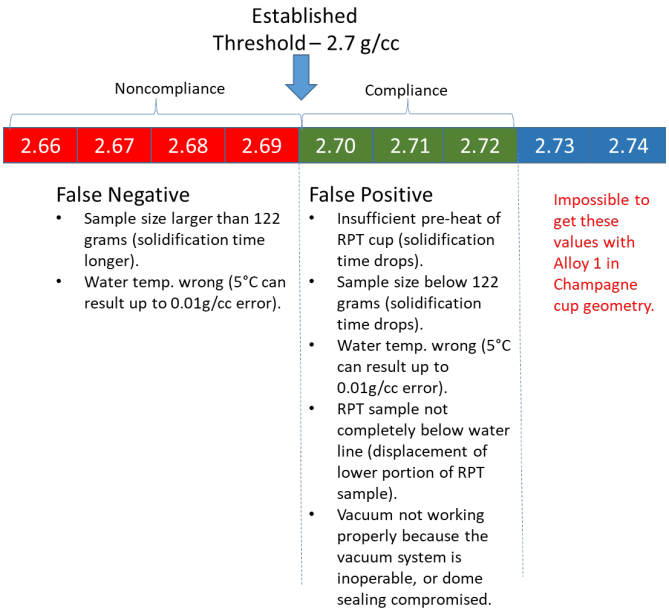

Figure 9. Summary of the known factors which can affect an accurate reading when conducting the RPT sample collection.

False positives can be more difficult to confirm. From Figure 9 we can see many potential issues that can result in a false positive reading, but again should there be a concern with the RPT sample result, one should confirm that the pre-heat of the RPT cup and ladle were reasonable, that the RPT dry mass was within target, water temperature measurement was accurate, wet mass immersion was below the waterline, and finally that the vacuum was reading properly.

Finally, RPT samples must be labeled and stored should future examination be needed. The time length for storing RPT samples should at least cover the time from casting up to when casting product undergoes its final inspection at the customer. If salt and pepper porosity issues are flagged by the customer in final inspection, the supplier foundry is contacted to begin its root cause investigation. The foundry could re-check the stored RPT samples from the same day the suspect castings were made to confirm the original density readings. Should the density be confirmed follow through with both a dry density check of the samples and check the λ_2 in a key region of the RPT sample to ensure that solidification rates are as in Figure 6. Should the λ_2 values be lower than what is shown in Figure 6, but the dry mass was on target, means that adequate pre-heat for either the RPT cup or ladle was not sufficient. Conversely, if the dry mass was somewhat below the 122 grams target it will possibly also have a slightly lower λ_2 value in key locations. Both scenarios suggest, upon this postmortem, that the suspect castings were made with an RPT data result that was originally an overestimate.

CONCLUSIONS

The authors have outlined a method for the development of a well verified RPT density threshold for compliance, but also addressed a decision-based protocol on either side of an established threshold RPT to rule out false positives and false negatives during production.

To summarize the conclusions, the authors wish to respond to the three questions listed at the end of the literature review with the answers determined from this manuscript.

1. How does one establish the absolute density, especially for Al-Si-Cu alloys which have limited previous reference data? *The authors recommend using a pore-free sample, typically and OES sample, use the existing programmable balance unit, measure the absolute density. For Alloy 1 this was found to be 2.74 g/cc.*

2. As the absolute densities and freezing ranges for alloys within the Al-Si-Cu family are different, what factors are considered in establishing a production valid density threshold? *The authors used castings at two different RPT densities and after extensive metallurgical evaluation, found the threshold required to achieve compliant castings. This was found to be 2.70 g/cc. Or the acceptable range is 2.7 g/cc up to 2.74 g/cc. Note that from λ_2 array analysis of the RPT test sample the highest level achieved will be 2.72 g/cc due to solidification shrinkage associated with both the cup design and the freezing range of the alloy.*

3. Is there an understanding of what factors can control false positives or false negative results in terms of the density threshold (± 0.01 g/cc)? *The review of Figure 9 summarizes most of the known errors encountered with the reading of the density value for the aluminum RPT sample.*

REFERENCES

1. Francisco C. Robles-Hernandez, Jose Martin Herrera Ramirez, Robert Mackay, “Al-Si Alloys,” 1st ed.; Springer, Gewerbestrasse, Switzerland, pp. 237 (2017).
2. M.A. Gafur, M.N. Haque and K.N. Prabhu, “Effect of chill thickness and superheat on casting/chill interfacial heat transfer during solidification of commercially pure aluminum,” *J. Mater. Process. Technol.*, 133, (3), 257–265 (2003).
3. J.E. Gruzleski & B.M. Closset, “The Treatment of Liquid Aluminum-Silicon Alloys,” American Foundry Society, Inc., 256pp (1990).
4. J. Campbell, “10 Rules for Good Castings,” *Modern Casting*, pp. 36-39 (April, 1997).
5. J. Campbell, “Castings,” Butterworth Heinemann, pp. 234(1997).
6. Editor: J.R. Davis, "ASM Specialty Handbook: Aluminum & Aluminum Alloys," pp. 306 (1996).
7. J. Campbell, “An Overview of the Effects of Bifilms on the Structure and Properties of Cast Alloys,” *Metallurgical and Materials Transactions B*, vol. 37(6): 857-863 (Dec. 2006).
8. P.S. Mohanty, F.H. Samuel, J.E. Gruzleski, “Experimental Study on Pore Nucleation by Inclusions in Aluminum Castings,” *AFS Transactions*, Vol. 105, pp. 555-564 (1995).
9. D. Dispinar & J. Campbell, “Critical assessment of Reduced Pressure Test, Part 1: Porosity Phenomena,” *International Journal of Cast Metals Research*, vol 17 (5)pp. 280-286 (2004).
10. R. Mackay, G. Byczynski, A. Elsayed “Novel Approach to Thermal Processing Development for Precision Sand Casting Process (PSCP) in Aluminium 319 Alloy” AFS Transactions 2021, April 12th, 2021
11. R. MacKay & G. Byczynski, “The Use of the Weibull Statistical Method to Assess the Reliability of Cast Aluminum Engine Blocks made from Different Casting Processes,” *Shape Casting: the Fourth International Symposium 2011*, TMS (2011), (ISBN: 978-1-11802-937-4).